

Supporting Information

A zeolite CAN-type aluminoborate with gigantic 24-ring channels

Gao-Juan Cao,^{†a} Qi Wei,^a Jian-Wen Cheng,^{*b} Lin Cheng,^c and Guo-Yu Yang^{*a}

^a MOE Key Laboratory of Cluster Science, School of Chemistry, Beijing Institute of Technology, Beijing 100081, China. E-mail: ygy@bit.edu.cn

^b Key Laboratory of the Ministry of Education for Advanced Catalysis Materials, Institute of Physical Chemistry, Zhejiang Normal University, Jinhua, Zhejiang 321004, China. E-mail: jwcheng@zjnu.cn

^c School of Chemistry, Tianjin Normal University, Tianjin 300387, China.

[†]Present Address: Department of Applied Chemistry, School of Life Science, Fujian Agriculture and Forestry University, Fuzhou, Fujian 350002, China.

Experimental Section

Table S1. Crystal and structure refinement data for BIT-1.

Table S2. Select bond distances (Å) and angles (°) for BIT-1.

Table S3. Hydrogen bond lengths (Å) and bond angles (°).

Table S4. State energies (eV) of the L-CB and the H-VB of BIT-1.

Figure S1. Experimental and simulated PXRD patterns for BIT-1.

Figure S2. (a) Organic templates and water molecules are located within 9R and 8R channels; Polyhedral representation of the 24R (b), 9R (c) and 8R (d) openings, respectively.

Figure S3. Schematic representation of the connection between AlO_4 tetrahedra and B_5O_{10} clusters. Color code: AlO_4 tetrahedron, green; B_5O_{10} cluster, fuchsia.

Figure S4. TGA curve of BIT-1.

Figure S5. Optical diffuse reflectance spectrum for BIT-1.

Figure S6. (a) Band structure for $[\text{Al}(\text{B}_5\text{O}_{10})]^{2-}$ in BIT-1; (b) Total density of states and partial density of states of $[\text{Al}(\text{B}_5\text{O}_{10})]^{2-}$ in BIT-1. The Fermi level is set at 0 eV.

Figure S7. The IR spectrum of BIT-1.

Experimental Section

Synthesis of BIT-1. A mixture of H_3BO_3 (0.542 g, 9 mmol), $\text{Al}(i\text{-PrO})_3$ (0.124 g, 0.6 mmol) and MAS (4 mL) was stirred for 30 min, then *n*-propylamine (1 mL) was added, a homogeneous gel (pH = 9) was formed after stirring about 30 min. The gel was sealed in a 40 mL Teflon-lined stainless steel autoclave and heated at 170 °C for 7 days and then slowly cooled to room temperature. The pure colorless prismatic crystals were obtained by filtration, washed with distilled water, and dried in air (90% yield based on $\text{Al}(i\text{-PrO})_3$). The crystals gradually lose crystal shape, and the appearance of unknown phases in the water. Elemental analysis calcd (%) for $\text{C}_3\text{H}_{24}\text{N}_2\text{AlB}_5\text{O}_{15}$ (BIT-1): C 8.80, H 5.91, N 6.84; found: C 8.56, H 4.90, N 6.51. IR (KBr, cm^{-1}): 3397(m), 3134(m), 1647(m), 1453(s), 1345(s), 1252(s), 1097(m), 934(m), 857(s), 787(m), 694(m), 656(w), 594(w), 477(w) (Fig. S8).

A suitable single crystal with dimensions of $0.25 \times 0.15 \times 0.15 \text{ mm}^3$ was mounted on a Saturn 724 diffractometer with graphite-monochromated $\text{MoK}\alpha$ radiation ($\lambda = 0.71073 \text{ \AA}$) at 293 K. The structure was solved by direct methods and refined by full matrix least squares on F^2 using the SHELXTL-97 program.¹ The H atoms of O3W, O4W, O5W and O6W in BIT-1 have not been included in the final refinement, other hydrogen atoms were placed in calculated positions and allowed to ride on their parent atoms. All non-hydrogen atoms were refined anisotropically except O3W, O4W, O5W and O6W. This structure could be satisfactorily solved in the space group $P6_3$. The structure was checked for possible missing symmetry with PLATON. The high symmetry and large pore sizes of BIT-1 as well as disorders of the ammoniums and water molecules in the pores precluded the location of these molecules in the channel. The PLATON/SQUEESE program² was used to deal with the large voids of structure in the final structure refinement. According to the C,H,N elemental and thermogravimetric (TG) analyses, 1.5 protonated methylamine, 0.5 protonated *n*-propylamine and 5 water molecules are expected per formula. Crystallographic data and structural refinements are summarized in Table S1. CCDC 953421 contains the supplementary crystallographic data for this paper.

1 (a) G. M. Sheldrick, *SHELXS-97, Program for the Solution of Crystal Structure*, University of Göttingen 1997; (b) G. M. Sheldrick, *SHELXL-97, Program for the Refinement of Crystal Structure*, University of Göttingen 1997.

2 A. L. Spek, *J. Appl. Crystallogr.* **2003**, *36*, 7–13.

Table S1. Crystal and structure refinement data for BIT-1.

| | |
|---------------------------------|--|
| formula | $C_{1.33}H_{9.77}AlB_5N_{1.33}O_{10.88}$ |
| M_r | 299.70 |
| T (K) | 293(2) |
| crystal system | hexgonal |
| space group | $P6_3$ |
| a (Å) | 21.4013(8) |
| b (Å) | 21.4013(8) |
| c (Å) | 7.1696(5) |
| V (Å ³) | 2843.8(2) |
| Z | 6 |
| D_c (g cm ⁻³) | 1.050 |
| μ (mm ⁻¹) | 0.140 |
| $F(000)$ | 913 |
| crystal size (mm) | 0.25 × 0.15 × 0.15 |
| index ranges | 2.91-27.48 |
| GOF | 1.087 |
| collected reflcns | 22349 |
| unique reflcns (R_{int}) | 3425 (0.0432) |
| observed reflcns | 3168 |
| $[I > 2\sigma(I)]$ | |
| refined parameters | 196 |
| $R_1^a/wR_2^b [I > 2\sigma(I)]$ | 0.0532/ 0.1626 |
| R_1^a/wR_2^b (all data) | 0.0571/ 0.1664 |
| largest difference | 0.311/ -0.278 |
| peak/hole (e·Å ⁻³) | |

Table S2. Select bond distances (Å) and angles (°) for BIT-1.

| Bonds distances (Å) | | Bond distances (Å) | |
|---------------------|------------|--------------------|----------|
| Al-O(1) | 1.717(2) | B(3)-O(3) | 1.444(3) |
| Al-O(8)#1 | 1.734(2) | B(3)-O(7) | 1.466(4) |
| Al-O(5)#2 | 1.734(2) | B(3)-O(6) | 1.478(4) |
| Al-O(10)#3 | 1.735(2) | B(3)-O(4) | 1.485(4) |
| B(1)-O(1) | 1.344(3) | B(4)-O(8) | 1.347(4) |
| B(1)-O(3) | 1.359(3) | B(4)-O(7) | 1.362(3) |
| B(1)-O(2) | 1.390(3) | B(4)-O(9) | 1.385(4) |
| B(2)-O(5) | 1.330(3) | B(5)-O(10) | 1.333(4) |
| B(2)-O(4) | 1.347(3) | B(5)-O(6) | 1.363(3) |
| B(2)-O(2) | 1.405(3) | B(5)-O(9) | 1.387(4) |
| Angles (°) | | Angles (°) | |
| O(1)-Al-O(8)#1 | 108.14(12) | O(3)-B(3)-O(7) | 109.5(3) |
| O(1)-Al-O(5)#2 | 109.92(11) | O(3)-B(3)-O(6) | 109.2(2) |
| O(8)#1-Al-O(5)#2 | 112.22(13) | O(7)-B(3)-O(6) | 111.1(2) |
| O(1)-Al-O(10)#3 | 107.87(12) | O(3)-B(3)-O(4) | 111.0(2) |
| O(8)#1-Al-O(10)#3 | 109.09(12) | O(7)-B(3)-O(4) | 108.3(2) |
| O(5)#2-Al-O(10)#3 | 109.50(15) | O(6)-B(3)-O(4) | 107.7(2) |
| O(1)-B(1)-O(3) | 119.9(2) | O(8)-B(4)-O(7) | 119.1(3) |
| O(1)-B(1)-O(2) | 120.8(2) | O(8)-B(4)-O(9) | 121.4(2) |
| O(3)-B(1)-O(2) | 119.2(2) | O(7)-B(4)-O(9) | 119.5(3) |
| O(5)-B(2)-O(4) | 124.4(2) | O(10)-B(5)-O(6) | 123.3(3) |
| O(5)-B(2)-O(2) | 116.6(2) | O(10)-B(5)-O(9) | 117.5(2) |
| O(4)-B(2)-O(2) | 119.0(2) | O(6)-B(5)-O(9) | 119.2(3) |

Symmetry codes for BIT-1: #1: $y - 1, -x + y, z + 1/2$; #2: $-y + 1, x - y + 1, z$; #3: $y - 1, -x + y, z - 1/2$.

Table S3. Hydrogen bond lengths (Å) and bond angles (°)

| D-H...A | d(D-H) | d(H...A) | d(D...A) | <(DHA) |
|------------------------|--------|----------|-----------|--------|
| N(1A)-H(1AD)...O(7) | 0.89 | 1.95 | 2.839(4) | 173.9 |
| N(1A)-H(1AD)...O(8) | 0.89 | 2.46 | 2.965(4) | 116.7 |
| N(1A)-H(1AE)...O(4)#7 | 0.89 | 1.99 | 2.860(3) | 163.8 |
| N(1A)-H(1AF)...O(6)#10 | 0.89 | 2.05 | 2.899(4) | 157.7 |
| O(1W)-H(1WA)...O(10) | 0.84 | 2.50 | 3.181(14) | 139.4 |
| O(1W)-H(1WB)...O(9) | 0.84 | 2.50 | 3.081(13) | 127.2 |
| O(1W)-H(1WB)...O(1)#5 | 0.84 | 2.66 | 3.342(16) | 139.6 |
| N(1B)-H(1BA)...O(7) | 0.90 | 1.91 | 2.726(18) | 149.9 |
| N(1B)-H(1BB)...O(2W)#3 | 0.90 | 2.37 | 2.977(18) | 125.5 |
| N(1B)-H(1BC)...O(6)#10 | 0.90 | 2.22 | 2.983(17) | 142.9 |
| N(1B)-H(1BC)...O(8) | 0.90 | 2.58 | 3.114(15) | 118.6 |
| O(2W)-H(2WA)...O(10) | 0.85 | 2.34 | 3.024(12) | 137.5 |
| O(2W)-H(2WB)...O(9) | 0.85 | 2.35 | 2.971(10) | 130.7 |
| O(2W)-H(2WB)...O(1)#5 | 0.85 | 2.62 | 3.222(14) | 128.9 |

Symmetry codes for BIT-1: #3: $y - 1, -x + y, z - 1/2$; #5: $x - y + 1, x + 1, z - 1/2$; #7: $-x + 1, -y + 2, z - 1/2$; #10: $x, y, z - 1$.

Table S4. State energies (eV) of the L-CB and the H-VB of BIT-1.

| k -point | L-CB | H-VB |
|-----------------------|---------|---------|
| G(0.000,0.000,0.000) | 6.58401 | 0.13727 |
| A(0.000,0.000,0.500) | 7.48834 | 0.0835 |
| H(-0.333,0.667,0.500) | 7.57174 | 0.08659 |
| K(-0.333,0.667,0.000) | 6.69688 | 0.11846 |
| G(0.000,0.000,0.000) | 6.58401 | 0.13727 |
| M(0.000,0.500,0.000) | 6.65651 | 0.12386 |
| L(0.000,0.500,0.500) | 7.54937 | 0.08629 |
| H(-0.333,0.667,0.500) | 7.57174 | 0.08659 |

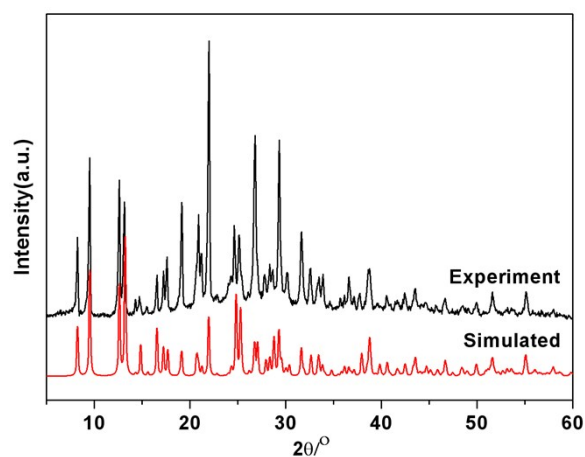


Figure S1. Experimental and simulated PXRD patterns for BIT-1.

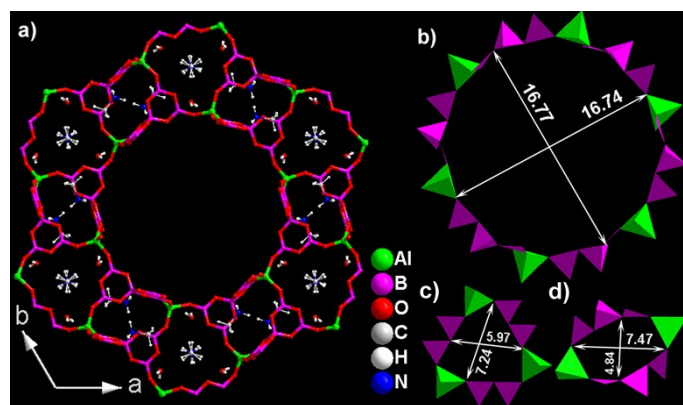


Figure S2. (a) Organic templates and water molecules are located within 9R and 8R channels; Polyhedral representation of the 24R (b), 9R (c) and 8R (d) openings, respectively.

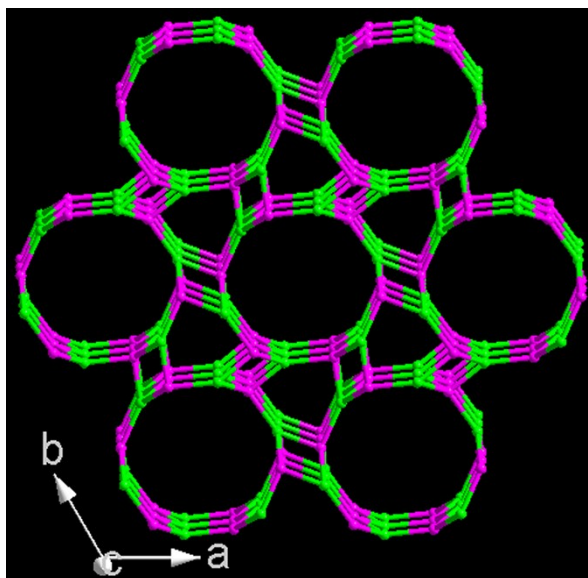


Figure S3. Schematic representation of the connection between AlO_4 tetrahedra and B_5O_{10} clusters. Color code: AlO_4 tetrahedron, green; B_5O_{10} cluster, fuchsia.

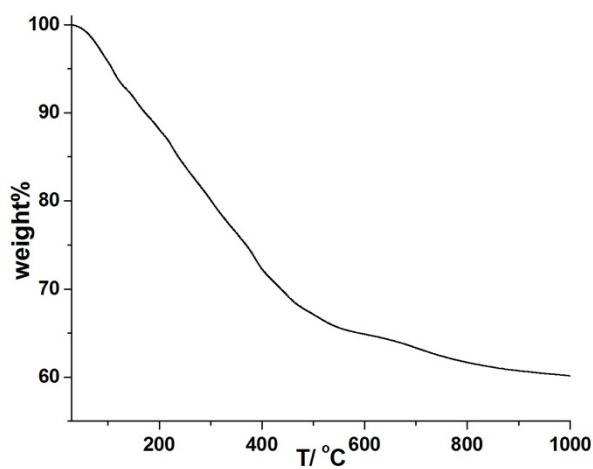


Figure S4. TGA curve of BIT-1.

The thermal behavior of BIT-1 was examined by TGA in a dry air atmosphere from 30 to 1000 °C with a heating rate of $10^\circ\text{C}\cdot\text{min}^{-1}$. TGA curve shows a gradual weight loss of 39.9% up to 1000 °C, which corresponding to the removal of all water molecules and ammoniums (calcd 41.1%). An PXRD study showed that the structure collapses after removal of the organic molecules, suggesting that the large-pore structure is unstable.

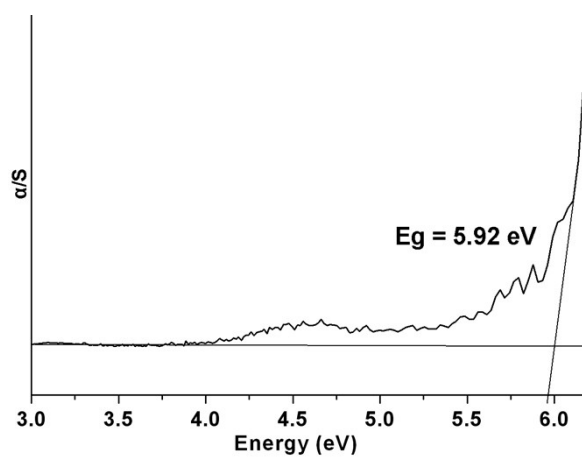


Figure S5. Optical diffuse reflectance spectrum for BIT-1.

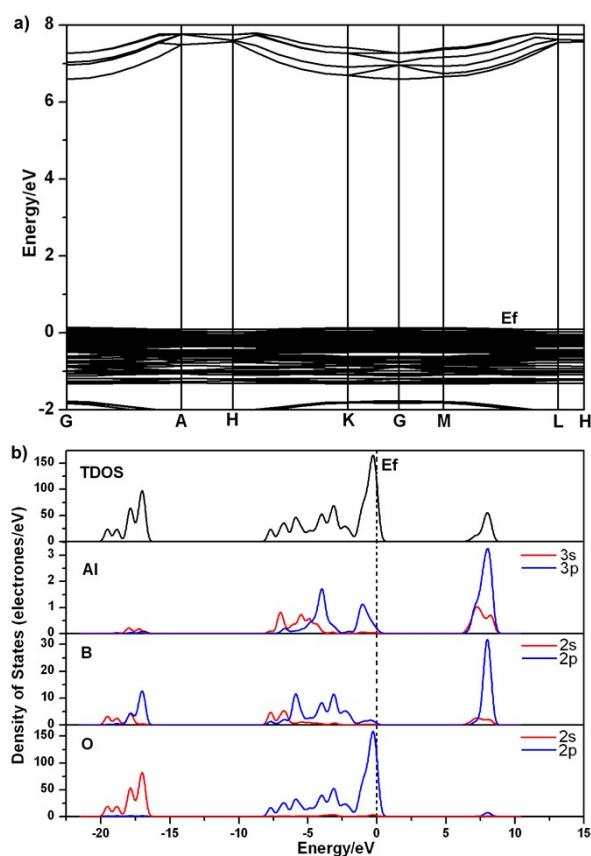


Figure S6. (a) Band structure for $[\text{Al}(\text{B}_5\text{O}_{10})]^{2-}$ in BIT-1; (b) Total density of states and partial density of states of $[\text{Al}(\text{B}_5\text{O}_{10})]^{2-}$ in BIT-1. The Fermi level is set at 0 eV. To further understand the chemical bonding in BIT-1, the band structure and densities of states (DOS) calculations for $[\text{Al}(\text{B}_5\text{O}_{10})]^{2-}$ in BIT-1 were made by using the

computer code CASTEP.³ It is necessary to mention that the calculations excluded the effects of the guest molecules. The top of the valence bands (VBs) and the bottom of the conduction bands (CBs) display dispersion for $[\text{Al}(\text{B}_5\text{O}_{10})]^{2-}$. Both the lowest energy (6.58 eV) of CBs and the highest energy (0.14 eV) of VBs are situated at the G point. Accordingly, $[\text{Al}(\text{B}_5\text{O}_{10})]^{2-}$ in BIT-1 shows a direct band gap of 6.45 eV. Its bands can be assigned according to total and partial DOS. The VBs from -22.5 to -17.0 are mainly derived from O-2s states. The bands from the -10 eV to the Fermi level are mainly contributions of O-2p and B-2p states. The CBs are dominated by unoccupied Al-3p and B-2p states.

3 M. D. Segall, P. J. D. Lindan, M. J. Probert, C. J. Pickard, P. J. Hasnip, S. J. Clark and M. C. Payne, *J. Phys.: Condens. Matter.*, **2002**, *14*, 2717–2744.

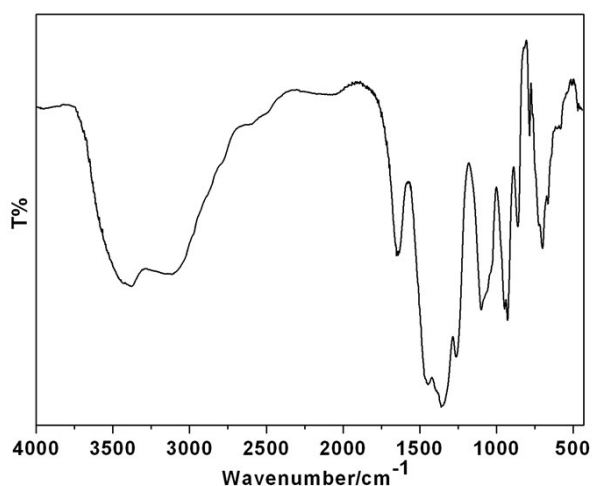


Figure S7. The IR spectrum of BIT-1.

The broad absorption bands in the range of $3400\text{--}3100\text{ cm}^{-1}$ in IR spectrum of BIT-1 are assigned as the characteristic peaks of O–H and N–H vibrations. The absorption peak at 1647 cm^{-1} is related to the asymmetric stretching vibrations and symmetric bond-bending vibrations of N–H and C–H bonds. The characteristic band around $1453\text{--}1252\text{ cm}^{-1}$ is due to the B–O asymmetric stretching of the BO_3 units. The band around $1097\text{--}934\text{ cm}^{-1}$ is associated with the BO_4 units. The presence of absorption peaks at 857 and 787 cm^{-1} originate from vibration of AlO_4 units.⁴

4 K. Nakamoto, *Infrared Spectra of Inorganic and Coordination Compounds*, Wiley, New York, **1970**.